AJNR

Differentiation of Primary Central Nervous System Lymphomas and Glioblastomas: Comparisons of Diagnostic Performance of Dynamic Susceptibility Contrast-Enhanced Perfusion MR Imaging without and with Contrast-Leakage Correction

C.H. Toh, K.-C. Wei, C.-N. Chang, S.-H. Ng and H.-F. Wong

AJNR Am J Neuroradiol 2013, 34 (6) 1145-1149
doi: https://doi.org/10.3174/ajnr.A3383
http://www.ajnr.org/content/34/6/1145

Differentiation of Primary Central Nervous System Lymphomas and Glioblastomas: Comparisons of Diagnostic Performance of Dynamic Susceptibility Contrast-Enhanced Perfusion MR Imaging without and with Contrast-Leakage Correction

C.H. Toh, K.-C. Wei, C.-N. Chang, S.-H. Ng, and H.-F. Wong

ABSTRACT

BACKGROUND AND PURPOSE: Contrast leakage results in underestimation of the CBV of brain tumors. Our aim was to compare the diagnostic performance of DSC perfusion MR imaging without and with mathematic contrast-leakage correction in differentiating PCNSLs and glioblastomas.

MATERIALS AND METHODS: Perfusion parameters—CBV, corrected CBV, and leakage coefficient—were measured in enhancing tumor portions and contralateral NAWM of 15 PCNSLs and 20 glioblastomas, respectively. The ratios of CBV and corrected CBV were calculated by dividing the tumor values by those obtained from contralateral NAWM. A paired *t* test was used to compare tumor K_2 and NAWM K_2, as well as tumor CBV ratios without and with leakage correction. Comparisons of CBV, corrected CBV, and K_2 between PCNSLs and glioblastomas were done by using a 2-sample *t* test. The diagnostic performance of DSC perfusion MR imaging without and with contrast-leakage correction was assessed with receiver operating characteristic curve analysis.

RESULTS: PCNSLs and glioblastomas demonstrated higher K_2 than those in their contralateral NAWM. Corrected CBV ratios were significantly higher than the uncorrected ones for both tumors. PCNSLs had lower CBV ratios ($P < .001$), lower corrected CBV ratios ($P < .001$), and higher K_2 ($P = .001$) compared with glioblastomas. In differentiating between PCNSLs and glioblastomas, the area under the curve of the CBV ratio, corrected CBV ratio, and K_2 were 0.984, 0.940, and 0.788, respectively.

CONCLUSIONS: PCNSL can be differentiated from glioblastoma with CBV ratios, corrected CBV ratios, and K_2. CBV without contrast-leakage correction seems to have the best diagnostic performance in differentiating the 2 tumors.

ABBREVIATIONS: DSC = dynamic susceptibility contrast-enhanced; K_2 = leakage coefficient; MPRAGE = magnetization-prepared rapid acquisition of gradient echo; NAWM = normal-appearing white mater; PCNSL = primary central nervous system lymphoma

Accurate distinguishing of PCNSLs from glioblastomas preoperatively is important for determination of appropriate treatment strategies.[1,2] Advanced imaging techniques such as DSC perfusion MR imaging complement the role of conventional MR imaging in differentiating the 2 tumors.[1,2] DSC perfusion MR imaging measures T2*-weighted signal-intensity loss occurring dynamically over bolus injection of contrast medium, from which relative CBV, a marker of tumor angiogenesis, can be computed.[3-5] On DSC perfusion MR imaging, PCNSLs demonstrate lower CBV compared with glioblastomas.[6-14]

In lesions with substantial BBB breakdown and contrast leakage, the T2*-weighted signal-intensity loss can be masked by signal-intensity increase secondary to T1 effects. In such instances, CBV will be underestimated.[3,15] To measure CBV with higher accuracy, a mathematic leakage-correction model has been proposed to process the DSC perfusion data.[15] It allows simultaneous assessment of tumor vascularity and vascular permeability by calculating leakage-corrected CBV and the leakage coefficient, respectively. In high-grade gliomas, the corrected CBV was found to have better correlation with tumor grade than the uncorrected one.[15] The K_2, on the other hand, was able to demonstrate the differences in vascular permeability among gliomas of different histologic grades.[16]

PCNSLs are also known to have increased vascular permeability.[17-19] Their low CBV and the characteristic intensity–time curve that went above the baseline were thought to be related to

Received July 9, 2012; accepted after revision August 31.

From the Departments of Medical Imaging and Intervention (C.H.T, S.-H.N, H.-F.W) and Neurosurgery (K.-C.W, C.-N.C), Chang Gung Memorial Hospital, Linkou and Chang Gung University College of Medicine, Tao-Yuan, Taiwan.

This work was partly supported by grants from the National Science Council Taiwan (NSC-98-2314-B-182A-051-MY3 to C.H. Toh). The authors also acknowledge support from Molecular Imaging Center, Chang Gung Memorial Hospital, Linkou, Taiwan.

Please address correspondence to Cheng Hong Toh, MD, Department of Medical Imaging and Intervention, Chang Gung Memorial Hospital, Linkou and Chang Gung University College of Medicine, No. 5, Fuxing St, Guishan Township, Taoyuan County 333, Taiwan; e-mail: eldomtoh@hotmail.com

http://dx.doi.org/10.3174/ajnr.A3383

high vascular permeability.[8,12] To the best of our knowledge, PCNSLs have never been studied with DSC perfusion MR imaging processed with the mathematic leakage-correction model.[6-13] Their corrected CBV and K_2 have also not been quantitatively compared with those of glioblastomas. In this study, we aimed to compare the diagnostic performance of DSC perfusion MR imaging without and with mathematic leakage correction in the differentiation of PCNSL and glioblastoma.

MATERIALS AND METHODS

Patients

Approval for this study was obtained from the institutional review board, and signed informed consent was obtained from all patients. Findings of preoperative MR imaging studies, obtained in 17 consecutive immunocompetent patients with PCNSL included in a prospective study, were reviewed. Images from 2 patients were excluded because of motion artifacts, so 15 patients (12 men, 3 women; mean age, 60.6 years; age range, 22–80 years) with PCNSL (mean size, 3.7 ± 1.6 cm) were analyzed. Findings of preoperative MR imaging studies, performed in 28 consecutive patients with glioblastomas in the same prospective study, were also reviewed. Three purely hemorrhagic and 5 cystic glioblastomas were excluded. Therefore, 20 patients (15 men, 5 women; mean age, 57.4 years; age range, 26–81 years) with glioblastomas (mean size, 4.5 ± 0.9 cm) were analyzed.

None of the patients had begun corticosteroid treatment, radiation therapy, or chemotherapy or had any previous brain biopsy at the time of MR imaging. Histologic diagnosis was obtained in all patients by surgical resection or biopsy. All the PCNSLs were diffuse large B-cell lymphomas. The estimated glomerular filtration rate was calculated from serum creatinine levels, patient demographics, and age. Patients with an estimated glomerular filtration rate < 60 mg/min/1.72 m^2 were excluded before enrollment.

MR Imaging

All MR imaging studies were performed by using a 3T unit (Magnetom Tim Trio; Siemens, Erlangen, Germany) by using a 12-channel phased-array head coil. Routine MR imaging pulse sequences included transverse T1WI, transverse T2WI, and transverse FLAIR. The DSC perfusion MR imaging was obtained with a T2*-weighted gradient-echo EPI sequence during the bolus injection of a standard dose (0.1 mmol/kg) of intravenous gadopentetate dimeglumine (Magnevist; Schering, Berlin, Germany). The injection rate was 4 mL/s for all patients and was immediately followed by a bolus injection of saline (total of 20 mL at the same rate). DSC perfusion MR imaging sequence parameters included the following: TR/TE, 1640/40 ms; flip angle, 90°; FOV, 230 × 230 mm; section thickness, 4 mm; 20 sections; and acquisition time of 1 minute 28 seconds. Fifty measurements were acquired allowing acquisition of at least 5 measurements before bolus arrival. No contrast agent was administered before DSC perfusion MR imaging. Postcontrast 3D MPRAGE images (TR/TE, 2000/2.63 ms; section thickness, 1 mm; inversion time, 900 ms; acquisition matrix, 224 × 256; and FOV, 224 × 256 mm) were acquired after completion of the DSC sequence.

Image Postprocessing

DSC perfusion MR imaging data were transferred to an independent workstation and processed by using the software nordicICE (Version 2.3; Nordic Imaging Lab, Bergen, Norway). For each voxel, the dynamic signal-intensity curve was converted to a relaxivity–time curve, a parameter related to the concentration of gadolinium in the voxel. The CBV was estimated by integrating the relaxivity–time curve.

Contrast-leakage correction was performed on the DSC images by using a technique outlined by Boxerman et al.[15] The method assumes that T1 shortening resulting from contrast leakage occurs in regions with disrupted BBB and uses linear fitting to determine the leakage coefficient, a first-order estimate of vascular permeability proportional to the leakage, the product of permeability and surface area. The K_2 was subsequently used for leakage correction and calculation of corrected CBV.

Image Analysis

The CBV, corrected CBV, and K_2 maps were coregistered to postcontrast MPRAGE on the basis of 3D nonrigid transformation and mutual information with the use of SPM2 software (Wellcome Department of Imaging Neuroscience, London, UK) before all imaging analysis.

On the basis of postcontrast MPRAGE, the enhancing portions of the entire tumor were segmented. A polygonal region of interest was first drawn to include the entire lesion on every section. A threshold pixel value was then manually chosen to create a scatter region of interest to segment the enhancing tumor portions. The segmented ROIs were subsequently used to measure the mean CBV, corrected CBV, and K_2 values of whole tumor, respectively. All ROIs did not include areas of necrosis or nontumor macrovessels evident on postcontrast MPRAGE.

For normalization, the ratios of CBV and corrected CBV were then calculated by dividing the tumor ROIs by the values obtained from a region of interest (size range, 30–50 mm^2) placed in the contralateral NAWM, respectively. The tumor K_2 values were not normalized because the NAWM K_2 values were equal or close to zero in most cases. Figures 1 and 2 illustrate the measurements of perfusion parameters in a PCNSL and a glioblastoma, respectively.

Statistical Analysis

For both PCNSLs and glioblastomas, a paired *t* test was used to compare tumor K_2 and NAWM K_2, as well as tumor CBV ratios without and with leakage correction. Between the PCNSL and glioblastoma groups, comparisons of CBV ratios, corrected CBV ratios, and K_2 values were performed by using a 2-sample *t* test. A commercially available statistical software package (Statistical Package for the Social Sciences 18; SPSS, Chicago, Illinois) was used for analysis, and *P* values $<.05$ indicated a statistically significant difference. Area under the curve and cutoff values of CBV ratios, corrected CBV ratios, and K_2 for distinguishing PCNSLs from glioblastomas were determined by receiver operating characteristic curve analysis. The cutoff values with the highest sensitivity and lowest false-positive rates were chosen for each perfusion parameter.

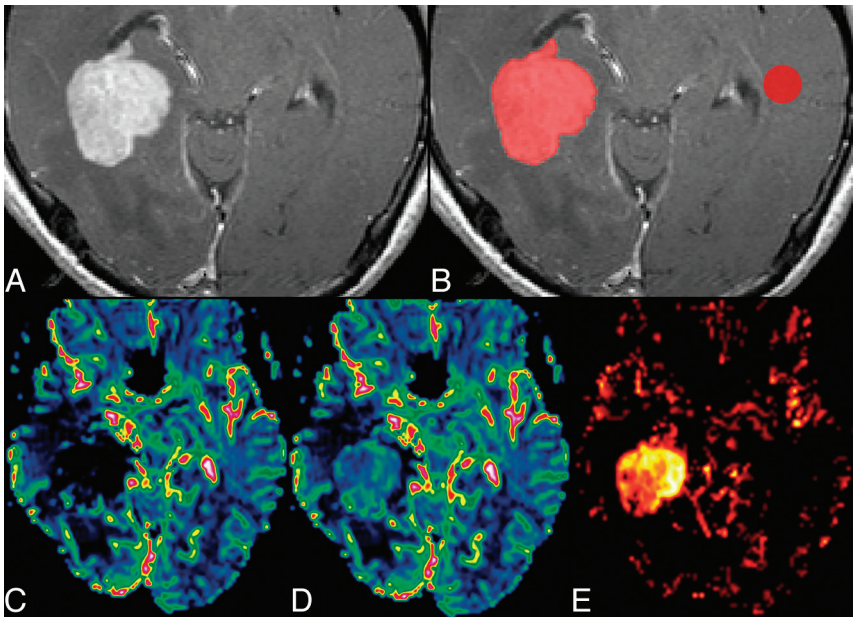

FIG 1. Measurements of perfusion parameters in a 22-year-old man with PCNSL. Axial contrast-enhanced MPRAGE (*A*) shows an enhancing mass in the right temporo-occipital region. *B*, On contrast-enhanced MPRAGE, 2 ROIs are placed, one over the entire enhancing tumor and another at the contralateral NAWM for the measurement of CBV (*C*), corrected CBV (*D*), and K_2 (*E*), respectively.

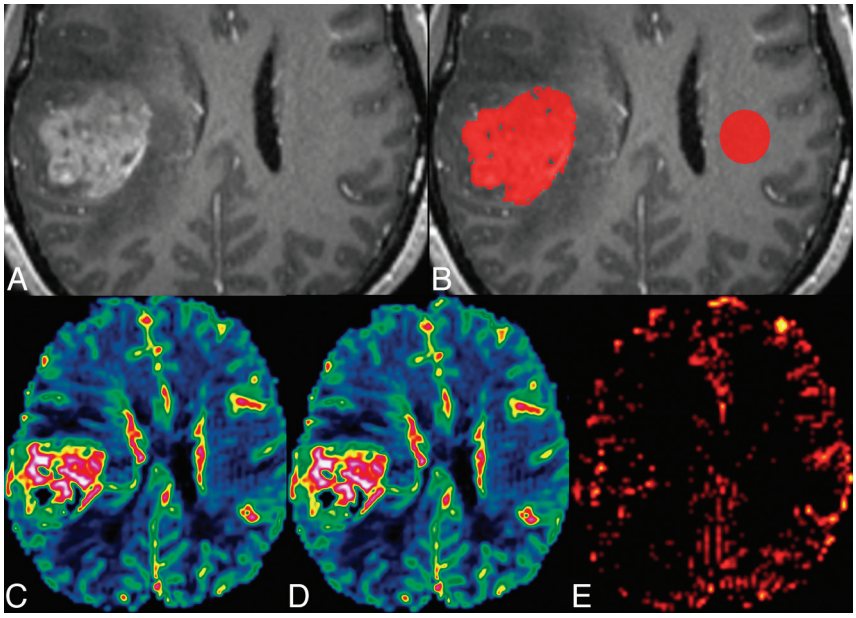

FIG 2. Measurements of perfusion parameters in a 40-year-old woman with glioblastoma. Axial contrast-enhanced MPRAGE (*A*) shows an enhancing mass in the right lateral frontal region. *B*, On contrast-enhanced MPRAGE, 2 ROIs are placed, one over the entire enhancing tumor and another at the contralateral NAWM for the measurement of CBV (*C*), corrected CBV (*D*), and K_2 (*E*), respectively.

Table 1: Quantitative comparisons of perfusion parameters between PCNSLs and glioblastomas[a]

Parameter	PCNSL	Glioblastoma	*P* Value	95% CI
CBV ratio	1.16 ± 0.66	5.01 ± 2.01	<.001	−4.82 to −2.84
Corrected CBV ratio	2.28 ± 0.60	5.47 ± 2.05	<.001	−4.19 to −2.18
K_2	1.88 ± 1.11	0.79 ± 0.68	.001	0.47–1.71

Note:—CI indicates confidence interval.

[a] Data are means.

RESULTS

The mean K_2 values were 1.88 ± 1.11 for PCNSLs and 0.02 ± 0.05 for their contralateral NAWM. The K_2 values were significantly higher in PCNSLs than in the contralateral NAWM ($P < .001$). The mean K_2 values were 0.79 ± 0.68 for glioblastomas and 0.01 ± 0.02 for their contralateral NAWM. Glioblastomas demonstrated significantly higher K_2 ($P < .001$) compared with their contralateral NAWM.

The mean CBV ratio and corrected CBV ratio were 1.16 ± 0.66 and 2.28 ± 0.60, respectively, for PCNSLs and were 5.00 ± 2.00 and 5.47 ± 2.05, respectively, for glioblastomas. The differences between the mean ratios of CBV and corrected CBV were statistically significant for both PCNSL ($P < .001$) and glioblastoma ($P < .001$). Table 1 shows the results of quantitative comparisons of the perfusion parameters between PCNSLs and glioblastomas. PCNSLs have a significantly lower CBV ratio ($P < .001$), a lower corrected CBV ratio ($P < .001$), and a higher K_2 ($P = .001$) compared with glioblastomas. On receiver operating characteristic curve analysis (Fig 3), the areas under the curve were 0.984 for the CBV ratio, 0.940 for corrected the CBV ratio, and 0.788 for K_2. The diagnostic accuracies of the CBV ratio, the corrected CBV ratio, and K_2 were 94.2%, 91.4%, and 77.1%, respectively. The results of receiver operating characteristic curve analysis are summarized in Table 2. When we differentiated PCNSLs from glioblastomas, CBV without leakage correction had the highest area under the curve and accuracy.

DISCUSSION

Our study shows that PCNSLs demonstrated significantly lower CBV ratios, lower corrected CBV ratios, and higher K_2 compared with glioblastomas. These differences indicate different tumor perfusion characteristics that allow discrimination of PCNSLs from glioblastomas.

In the present study, PCNSLs and glioblastomas demonstrated K_2 higher than that measured in NAWM, which suggested that there was an increase of vascular permeability in both tumors. However, the degree of K_2 increase was different between PCNSLs and glioblastomas. The higher K_2 in PCNSLs indi-

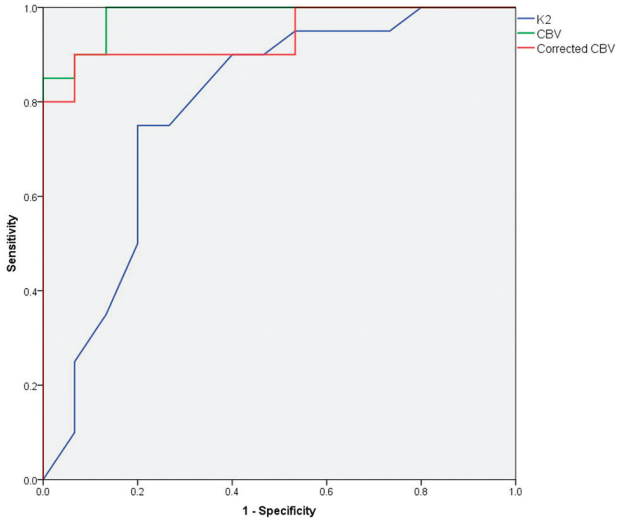

FIG 3. Receiver operating characteristic curve analysis for comparisons of the diagnostic performance of CBV, corrected CBV, and K_2.

cated that there was a greater degree of BBB disruption and thus higher vascular permeability in PCNSLs compared with glioblastomas. In the past, comparisons of the vascular permeability between PCNSLs and glioblastomas based on quantification of the permeability surface area product or volume transfer constant (K^{trans}) had only been performed with perfusion CT,[18,20] yielding results that were controversial. The higher vascular permeability in PCNSLs as demonstrated in the present study is in agreement with that reported by Warnke et al.[18] Our results suggested that K_2 derived from DSC perfusion MR imaging may serve as a quantitative marker of vascular permeability. On electron microscopy, ultrastructural changes associated with increased vascular permeability, such as thinned endothelial cells, fenestrations in capillary endothelium, and absence of endothelium between the lumen and basement membrane, were present in PCNSLs.[17]

The BBB was particularly absent in PCNSLs associated with vascular endothelial growth factor expression.[19] Therefore, the high K_2 in PCNSLs may reflect the presence of these vascular ultrastructures that lead to increased vascular permeability. However, due to the complex relationship between contrast agent concentration in tissue and the measured change in signal intensity, K_2 may not correlate linearly with the underlying permeability.[15] A positive relationship between K_2 and the K^{trans} may only exist with high flip angles.[21] In our study protocol, the DSC perfusion data were acquired with a flip angle of 90° and that has allowed comparison of the K_2 between the 2 tumors.

In this study, CBV ratios of PCNSL were lower than those of glioblastomas, a finding that is in agreement with those reported in the literature.[6,7,9,10] Two factors might contribute to the lower CBV in PCNSL. First, neovascularization is not a prominent histologic feature in PCNSL. In 1 study, PCNSLs were found to have lower CBV on DSC perfusion MR imaging and lower microvessel density on histologic analysis compared with high-grade gliomas.[10] In gliomas, there was a positive correlation between microvessel density and CBV.[22] Although this correlation has not been investigated with regard to PCNSLs, we speculate that the lower microvessel density might be related to the lower tumor CBV in PCNSL. Second, the high vascular permeability in PCNSL, as shown with high K_2 values, probably resulted in tumor CBV that was underestimated before leakage correction.

The significant increase of CBV following contrast-leakage correction in PCNSLs and glioblastomas may imply greater accuracy in CBV measurement. However, in terms of differentiation of the 2 tumors, we found no added value of the contrast-leakage correction. The diagnostic accuracy of corrected CBV was, in fact, lower than the accuracy without leakage correction. The differences in vascular permeability may result in a different degree of CBV correction in PCNSLs and glioblastomas. The greater restoration of CBV in PCNSL, which has higher vascular permeability, has decreased the CBV differences between the 2 tumors, and that decrease may indirectly lead to the lower diagnostic accuracy of corrected CBV.

The signal-intensity time curve of DSC perfusion MR imaging can also be described with percentage of signal recovery,[12,23] which represents the percentage of signal-intensity recovery at the end of the first pass and can be calculated without complex modeling or a sophisticated leakage-correction algorithm. The percentage of signal recovery can be measured simply by moving the region of interest within the tumors on a workstation. Mangla et al[12] reported that percentage of signal recovery was significantly higher in PCNSL compared with glioblastoma, and it was even better than CBV in differentiating PCNSLs from glioblastoma and metastases. However, there are some limitations with the percentage of signal recovery. Although the measurement of percentage of signal recovery is simple, it is associated with inherent subjectivity in the determination of region of interest. While tumor CBV has been shown to be related to angiogenesis, the physiologic basis of the percentage of signal recovery remains unclear. The relationship between percentage of signal recovery and permeability is also controversial. An early study proposed that the high percentage of signal recovery was due to high permeability.[8] However, recent studies suggested that the high percentage of signal recovery may indicate lower permeability.[12,23] Finally, the percentage of signal recovery of different portions of a tumor cannot be visualized simultaneously because percentage of signal recovery is not displayed in a voxelwise basis on a parametric map; therefore, it is not as straightforward and convenient as CBV and K_2 maps.

Table 2: ROC of CBV, corrected CBV, and K_2 in differentiating PCNSLs from glioblastomas[a]

Parameter	AUC	95% CI	*P* Value	CV	SEN	SPE	Accuracy
CBV ratio	0.984	0.952–1.000	<.001	1.88	100	86.7	94.2
Corrected CBV ratio	0.940	0.861–1.000	<.001	3.01	90	93.3	91.4
				2.08	100	46.7	77.1
K_2	0.788	0.624–0.953	.004	1.2	75	80.0	77.1

Note:—CI indicates confidence interval; CV, cutoff value; SEN, sensitivity; SPE, specificity; AUC, area under the curve; ROC, receiver operating characteristic curve analysis.
[a] Data of sensitivity, specificity, and accuracy are in percentages.

There are several methods for correcting the T1 effects associated with contrast leakage during CBV calculation. Preload contrast medium administration and mathematic leakage correction are 2 different approaches. A recent study showed that the 2 methods had a synergistic effect and that combining the 2 improved the accuracy and precision of CBV measurement.[24] In the present study, preload contrast medium was not administered for several reasons. First, there is still no consensus on whether preload contrast medium should be administered routinely. Second, there is no guideline or recommendation on the dose of preload contrast medium. Third, the relationship between contrast medium dose and the degree of T1 effect saturation is also unclear. Finally, improved accuracy and precision in CBV measurement do not imply better diagnostic performance. It is possible that the diagnostic performance of DSC perfusion MR imaging, which appears to become lower after mathematic leakage correction as shown in our study, may be further reduced by preload contrast medium administration. However, to determine the effect of preload contrast medium, future studies will have to perform DSC perfusion MR imaging during the preload injection to get the uncorrected CBV and then perform a second injection to obtain preloaded DSC perfusion data for leakage-corrected CBV.

Our study is limited by lack of direct correlations between perfusion parameters and histologic features such as microvessel density and endothelial ultrastructure. Moreover, there are many factors, including vascular surface area; vascular permeability; blood flow; and hydrostatic, interstitial, and osmotic gradients across the endothelium, that affect leakiness of vasculature. The K_2 measured with DSC perfusion MR imaging reflects the summation effect of all these factors on vascular leakiness. Because in vivo quantification of the individual effect of each factor is currently not feasible, we could not definitely state that the changes in K_2 were solely due to the changes in vascular permeability.

CONCLUSIONS

PCNSLs demonstrated significantly lower CBV, lower corrected CBV, and higher K_2 compared with glioblastomas. These differences may imply lower tumor vascularity and higher vascular permeability in PCNSL. Their different perfusion characteristics allowed discrimination of PCNSL from glioblastoma. CBV without contrast-leakage correction seems to have the best diagnostic performance in differentiating the 2 tumors. *Money paid to the Institution.

REFERENCES

1. Haldorsen IS, Espeland A, Larsson EM. **Central nervous system lymphoma: characteristic findings on traditional and advanced imaging.** *AJNR Am J Neuroradiol* 2011;32:984–92
2. Toh CH, Castillo M, Wong AM, et al. **Primary cerebral lymphoma and glioblastoma multiforme: differences in diffusion characteristics evaluated with diffusion tensor imaging.** *AJNR Am J Neuroradiol* 2008;29:471–75
3. Zaharchuk G. **Theoretical basis of hemodynamic MR imaging techniques to measure cerebral blood volume, cerebral blood flow, and permeability.** *AJNR Am J Neuroradiol* 2007;28:1850–58
4. Cha S. **Update on brain tumor imaging: from anatomy to physiology.** *AJNR Am J Neuroradiol* 2006;27:475–87
5. Provenzale JM, Mukundan S, Barboriak DP. **Diffusion-weighted and perfusion MR imaging for brain tumor characterization and assessment of treatment response.** *Radiology* 2006;239:632–49
6. Sugahara T, Korogi Y, Shigematsu Y, et al. **Perfusion-sensitive MRI of cerebral lymphomas: a preliminary report.** *J Comput Assist Tomogr* 1999;23:232–37
7. Cho SK, Na DG, Ryoo JW, et al. **Perfusion MR imaging: clinical utility for the differential diagnosis of various brain tumors.** *Korean J Radiol* 2002;3:171–79
8. Hartmann M, Heiland S, Harting I, et al. **Distinguishing of primary cerebral lymphoma from high-grade glioma with perfusion-weighted magnetic resonance imaging.** *Neurosci Lett* 2003;338:119–22
9. Calli C, Kitis O, Yunten N, et al. **Perfusion and diffusion MR imaging in enhancing malignant cerebral tumors.** *Eur J Radiol* 2006;58:394–403
10. Liao W, Liu Y, Wang X, et al. **Differentiation of primary central nervous system lymphoma and high-grade glioma with dynamic susceptibility contrast-enhanced perfusion magnetic resonance imaging.** *Acta Radiol* 2009;50:217–25
11. Lee IH, Kim ST, Kim HJ, et al. **Analysis of perfusion weighted image of CNS lymphoma.** *Eur J Radiol* 2010;76:48–51
12. Mangla R, Kolar B, Zhu T, et al. **Percentage signal recovery derived from MR dynamic susceptibility contrast imaging is useful to differentiate common enhancing malignant lesions of the brain.** *AJNR Am J Neuroradiol* 2011;32:1004–10
13. Wang S, Kim S, Chawla S, et al. **Differentiation between glioblastomas, solitary brain metastases, and primary cerebral lymphomas using diffusion tensor and dynamic susceptibility contrast-enhanced MR imaging.** *AJNR Am J Neuroradiol* 2011;32:507–14
14. Ma JH, Kim HS, Rim NJ, et al. **Differentiation among glioblastoma multiforme, solitary metastatic tumor, and lymphoma using whole-tumor histogram analysis of the normalized cerebral blood volume in enhancing and perienhancing lesions.** *AJNR Am J Neuroradiol* 2010;31:1699–706
15. Boxerman JL, Schmainda KM, Weisskoff RM. **Relative cerebral blood volume maps corrected for contrast agent extravasation significantly correlate with glioma tumor grade, whereas uncorrected maps do not.** *AJNR Am J Neuroradiol* 2006;27:859–67
16. Server A, Graff BA, Orheim TE, et al. **Measurements of diagnostic examination performance and correlation analysis using microvascular leakage, cerebral blood volume, and blood flow derived from 3T dynamic susceptibility-weighted contrast-enhanced perfusion MR imaging in glial tumor grading.** *Neuroradiology* 2011;53:435–47
17. Molnár PP, O'Neill BP, Scheithauer BW, et al. **The blood-brain barrier in primary CNS lymphomas: ultrastructural evidence of endothelial cell death.** *Neuro Oncol* 1999;1:89–100
18. Warnke PC, Timmer J, Ostertag CB, et al. **Capillary physiology and drug delivery in central nervous system lymphomas.** *Ann Neurol* 2005;57:136–39
19. Takeuchi H, Matsuda K, Kitai R, et al. **Angiogenesis in primary central nervous system lymphoma (PCNSL).** *J Neurooncol* 2007;84:141–45
20. Schramm P, Xyda A, Klotz E, et al. **Dynamic CT perfusion imaging of intra-axial brain tumours: differentiation of high-grade gliomas from primary CNS lymphomas.** *Eur Radiol* 2010;20:2482–90
21. Emblem KE, Mouridsen K, Borra RJ, et al. **Does DSC-derived CA extravasation correlate with DCE K^{trans}?** In: *Procedures of the International Society of Magnetic Resonance in Medicine,* Montreal, Quebec, Canada. May 6–13, 2011;1:791
22. Sadeghi N, D'Haene N, Decaestecker C, et al. **Apparent diffusion coefficient and cerebral blood volume in brain gliomas: relation to tumor cell density and tumor microvessel density based on stereotactic biopsies.** *AJNR Am J Neuroradiol* 2008;29:476–82
23. Cha S, Lupo JM, Chen MH, et al. **Differentiation of glioblastoma multiforme and single brain metastasis by peak height and percentage of signal intensity recovery derived from dynamic susceptibility-weighted contrast-enhanced perfusion MR imaging.** *AJNR Am J Neuroradiol* 2007;28:1078–84
24. Boxerman JL, Prah DE, Paulson ES, et al. **The role of preload and leakage correction in gadolinium-based cerebral blood volume estimation determined by comparison with MION as a criterion standard.** *AJNR Am J Neuroradiol* 2012;33:1081–87